Journal of Ultrasound (2021) 24:241–247
https://doi.org/10.1007/s40477-020-00511-5

REVIEW PAPER

Diagnostic imaging of parotid gland oncocytoma: a pictorial review with emphasis on ultrasound assessment

Antonio Corvino[1,7] · Martina Caruso[2] · Carlo Varelli[3] · Francesca Di Gennaro[4] · Saverio Pignata[5] · Fabio Corvino[6] · Gianfranco Vallone[2] · Orlando Catalano[3]

Received: 18 May 2020 / Accepted: 13 July 2020 / Published online: 24 July 2020

Abstract

Parotid gland oncocytoma (PGO) is a rare benign epithelial tumor that usually occurs in the elderly population. The most common clinical presentation is a painless, slow-growing, non-tender, lobulated, and mobile mass. Histologically, it is composed of monotonous sheets of epithelial cells (oncocytes) with a central scar. The cross-sectional appearance is not specific, and it overlaps with other parotid lesions. On ultrasound (US), oncocytoma appears as an ovoid, well-defined, homogeneous, and hypoechoic lesion. Cystic and hemorrhagic areas as well as intralesional fat may be observed. Doppler analysis shows intratumoral vessels, sometimes with a spoke-wheel pattern. The peak systolic flow is high (up to 100 cm/sec). Furthermore, oncocytoma is avid of FDG on a PET scan, as well as a malignant tumor. Thus, a combined clinical, imaging, and pathologic assessment is essential to establish the most accurate diagnosis and plan the best treatment. US, combined with Doppler techniques, can play an important role in suggesting the diagnosis and confirming it through percutaneous sampling. The purpose of this review is to show the imaging findings in PGO, with special emphasis on the US appearance.

Keywords Oncocytoma · Parotid gland · Tumor · Ultrasound · Color doppler

Introduction

Oncocytoma of the salivary glands—first described by Jaffé in 1932 and also called oncocytic adenoma, oxyphilic granular cell adenoma, or oxyphilic adenoma—is a benign epithelial tumor usually diagnosed in the sixth to eighth decades [1]. Although no strong sex predilection exists, evidence shows that women tend to be more commonly affected [2]. Oncocytomas are considered rare, representing less than 1% of all salivary gland tumors, involving mainly the parotid gland (78%), rarely minor salivary glands located in the larynx, tonsillar fossa, and lacrimal gland. This tumor also arises in other organs, such as the kidney, adrenal, thyroid, and pituitary glands [3]. In 7% of oncocytoma cases, parotid gland oncocytoma (PGO) is multifocal or bilateral [3, 4].

Physical examination usually reveals a painless, slow-growing, non-tender, firm, lobulated, and mobile mass, but sometimes the patient refers to a clinician for the development of pain and/or facial nerve paralysis [4]. Such symptoms were initially regarded as criteria of malignancy but later were observed in combination with benign tumors, such as Warthin's tumor, pleomorphic adenoma, lipoma, and PGO [5]. Necrosis, inflammation, spontaneous hemorrhage,

✉ Antonio Corvino
an.cor@hotmail.it

1 Motor Science and Wellness Department, University of Naples "Parthenope", via F. Acton 38, I-80133 Naples, Italy

2 Advanced Biomedical Sciences Department, University Federico II of Naples (UNINA), via S. Pansini 5, 80131 Naples, Italy

3 Radiology Unit, Varelli Institute, via Cornelia dei Gracchi 65, 80126 Naples, Italy

4 Nuclear Medicine Division, Radiology and Radiotherapy Department, National Cancer Institute Pascale Foundation, via M. Semmola 53, 80131 Naples, Italy

5 Ultrasound Unit, Ninetta Rosano Institute, via Capo Tirone 14, 87021 Belvedere Marittimo (CS), Italy

6 Vascular and Interventional Radiology Department, Cardarelli Hospital, via A. Cardarelli 9, 80131 Naples, Italy

7 Casal di Principe, Italy

and fibrosis can cause compression, ischemia, and strangulation of the facial nerve, resulting in peripheral paralysis [5].

PGO represents a diagnostic challenge, given its low prevalence and the lack of high specific imaging findings. To our knowledge, the literature comprises only anecdotal case reports and small case series. The aim of this review is to summarize the imaging findings in PGO and its differential diagnosis, with emphasis on ultrasound (US) assessment.

Pathology

The World Health Organization (WHO) defines three categories of salivary gland oncocytic neoplasms: nodular oncocytic hyperplasia or oncocytosis, oncocytoma, and oncocytic carcinoma. The first one is a multifocal process in which the glandular parenchyma is progressively replaced by oncocytic lobules, with small foci of residual serous glands and ducts. Oncocytoma is the most common occurrence, histologically composed of monotonous sheets of epithelial cells (oncocytes) with a central scar. Oncocytic carcinoma is the rarest of the oncocytic neoplasms, associated with a preexisting oncocytoma or raising de novo [6]. The oncocytes are enlarged polygonal cells with granular intensely eosinophilic cytoplasm, a round uniform nucleus, and a low nucleus–cytoplasm ratio. Such features are associated with marked mitochondrial hyperplasia and the paucity of other organelles, probably resulting from mitochondrial dysfunction and defective cellular metabolism [7]. The risk factors of oncocytomas are yet unknown, but a history of radiation exposure five or more years prior to presentation has been noted in 20% of cases [8].

Imaging features

Ultrasound

US is the first-line examination method to assess salivary gland abnormalities, owing to their relatively superficial position [9]. This technique enables differentiation solid from cystic masses with high reliability (98% confidence interval) [10, 11]. Furthermore, color and power Doppler have improved the diagnostic utility of US by providing a real-time evaluation of vascularity, which can supply important differential diagnostic data and suggest the final diagnosis with high diagnostic confidence [10].

Modern high-resolution transducers provide salivary gland images with excellent spatial and contrast resolution [12, 13]. When they are unavailable, the application of spacer pads or a huge amount of free gel can be particularly helpful in the B-mode and color Doppler assessment of highly superficial lesions [14]. The US examination of the parotid gland should be carried out with the highest frequency transducer available. Usually, 7–12 MHz wideband linear transducers are employed. Lower frequencies (5–10 MHz) are preferred to assess large tumors or lesions located in the deep aspect of the gland [15]. Parotid lesions have to be evaluated in at least two perpendicular planes during the exam, which should be completed with the assessment of neck lymph nodes to search for concomitant or related diseases [9].

The parotid gland is located in the retromandibular fossa, anterior to the ear and sternocleidomastoid muscle. It consists of a superficial lobe and a deep one, separated by a plane in which the facial nerve and its branches run. Parts of the nerve trunk may be visualized only with high-frequency probes (13–18 MHz) and appear as a hyperechoic binary structure. Its branches are not visible on US. Therefore, the retromandibular vein, which usually lies directly above the trunk of the facial nerve, is used as a landmark separating the superficial and deep lobes of the parotid glands [9, 15]. This aspect should be considered when imaging parotid tumors, highlighting to the surgeon the possible extent of a superficial tumor into the deep lobe. The deep lobe cannot be explored entirely on US, given the acoustic shadow behind the mandibular ramus. Parotid glands must be bilaterally investigated since many diseases occur bilaterally [10]. Normal glandular echogenicity is generally homogeneous and varies from very bright and markedly hyperechoic to only slightly hyperechoic in comparison to adjacent muscles, depending on the amount of intraglandular fatty tissue. US waves are markedly suppressed in case of high fat content, so the deep lobe is not always accessible, and sometimes even large vessels crossing the gland, such as the retromandibular vein, are barely visible or not visible at all on gray-scale images [9]. Intraparotid lymph nodes may be observed, mainly in the upper and lower poles of the superficial part of the gland. They appear to be oval, with a short axis of less than 5–6 mm and a hyperechoic hilum. The US assessment of a solid lesion should include Doppler evaluation by comparing the vessel density in the nodule with the normal parenchyma and measuring the peak systolic flow [9].

Although some aspects may raise suspicion, the US features of oncocytoma are nonspecific. PGO appears as an ovoid, well-defined, sometimes lobulated, and homogeneously hypoechoic mass [4]. The echotexture can be inhomogeneous because of cystic and hemorrhagic areas or intralesional fat, which appears echogenic. The central scar is not visible on US. The literature on the vascular pattern of PGOs is limited. In our experience, we noted that these tumors are usually quite vascularized. Vascular structures have a diffuse intralesional distribution, and the peak systolic flow is quite high (up to 100 cm/sec) (Figs. 1, 2, and 3). Sometimes a spoke-wheel pattern is observed (Fig. 4). This vascular pattern recalls what is sometimes visible in renal oncocytoma: the vessel branches extend from the periphery to the central

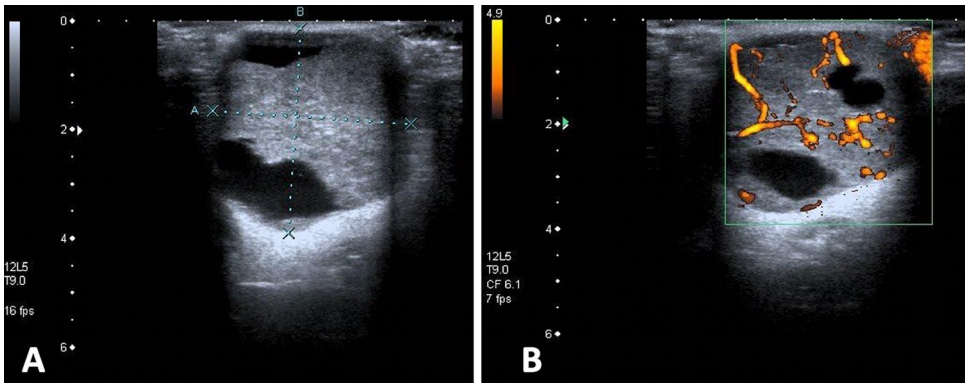

Fig. 1 B-mode **a** and power Doppler **b** scans of the parotid gland. Oval, well-defined oncocytoma with slightly hyperechoic echotexture compared to glandular parenchyma and some cystic anechoic areas. Power Doppler shows intralesional vessels

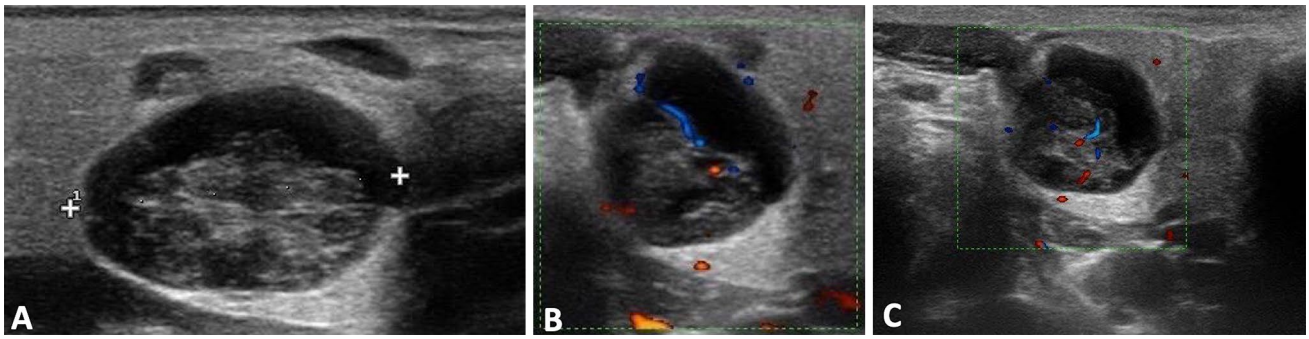

Fig. 2 B-mode **a** and color Doppler **b** and **c** scans of the parotid gland. Oval nodule with well-defined margins and some cystic areas. Color Doppler shows vascular signals inside the solid component

portion of the mass, supplying it centripetally [16]. Although the color Doppler features of PGOs are not pathognomonic, the presence of a spoke-wheel appearance and/or a high peak systolic flow should suggest a possible diagnosis.

US PGO features overlap with those of pleomorphic adenoma, which is the most common parotid tumor, usually occurring in adults older than forty years, with a slight predominance among women. Pleomorphic adenoma is described as an oval or round, homogeneously hypoechoic, and well-defined mass. Its margins are more often lobulated than those of oncocytoma. Dystrophic calcifications are common and represent a relatively specific imaging finding usually absent in oncocytic neoplasm [1]. Larger lesions may appear inhomogeneous, poorly defined, and with cystic degeneration [17]. The vascularization is usually moderate with complete or incomplete capsular branches and a single internal and generally venous vascular pole [9]. The peak systolic velocities are usually lower than 25 cm/sec [18]. The differential diagnosis between PGO and pleomorphic adenoma can be difficult on B-mode grayscale because the US findings overlap, but color and power Doppler are helpful.

Limited evidence is currently available on the use of contrast-enhanced ultrasound (CEUS) and elastography as additional diagnostic tools for the evaluation of parotid masses, in particular of PGO [19, 20].

CEUS using a second-generation contrast agent allows the analysis of both macro- and microvascular blood flow. Microbubble-enhanced US can improve the detection of perfusion by depicting more vessels and more intense perfusion compared to color and power Doppler. Therefore, it could help identify the PGO spoke-wheel pattern or the diffuse intralesional vascular distribution. On the other hand, pleomorphic adenomas usually show weak or no vessels; sometimes strong peripheral and/or internal vessels could be observed [21]. So far, the EFSUMB do not recommend CEUS for the characterization of salivary gland lesions in clinical practice [22].

Also, elastography allows the subjective or objective stiffness pattern analysis of the lesion and surrounding tissues, whether soft or hard and homogeneous or heterogeneous. To our knowledge, no studies about PGO stiffness are available, but Liu et al. observed that benign and malignant parotid nodules have significant different stiffness [23]. Therefore, elastography could increase US accuracy in the identification of parotid benign lesions and may decrease the need of fine-needle aspiration cytology (FNAC) or core biopsy for these nodules.

Thus, further studies are needed to confirm these preliminary results regarding parotid nodules and to

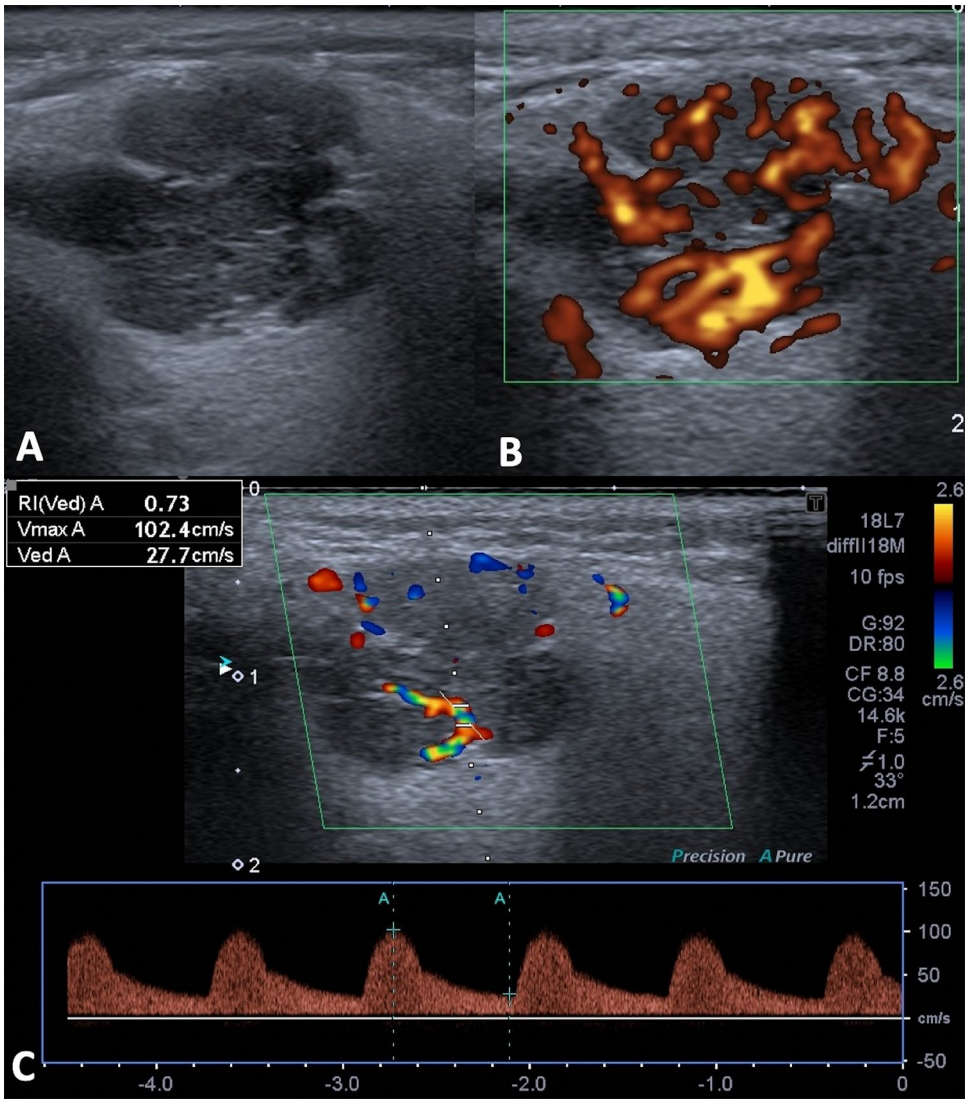

Fig. 3 B-mode **a** power Doppler **b** and spectral Doppler **c** scans of the parotid gland. Well-defined, lobulated, and hypoechoic oncocytoma with rich intralesional vascularization on power Doppler and high peak systolic flow (102 cm/sec)

investigate the diagnostic role of CEUS and elastography in PGO evaluation.

Radiological and nuclear imaging

Computed tomography (CT) and magnetic resonance imaging (MRI) are useful in preoperative planning by offering panoramic views of the examined subject. They are strongly recommended when the deep aspect of any parotid mass is not clearly visualized on US. They are also suggested in case of a suspected malignant lesion to examine the entire lesion and deep-lying lymph nodes to assess possible infiltration of bones or deep structures, such as the base of the skull as well as the parapharyngeal space, and to establish the relationship of the lesion with the facial nerve [9, 17, 24]. It is relevant to highlight that CT and MRI usually do not increase the specificity of US. Hence, when a well-circumscribed nodule in the superficial lobe of the parotid is found, cytological or bioptic sampling should be preferred to cross-sectional imaging.

The CT features of PGOs are represented by a well-defined, homogeneous enhancing tumor with a non-enhancing curvilinear cleft (central scar composed of hyalinized and fibrous tissue) or cystic component and a "deformable" appearance in the case of large lesions (contours distorted by surrounding structures) [1]. Differential diagnosis includes mainly Warthin's tumor, which appears as a well-defined mass, sometimes associated with cystic components. However, its post-contrast behavior is usually different (increased enhancement in the early phase and decreased in the delayed phase), and the non-enhancing central scar has not been reported in the literature [1].

The MRI appearance of PGO is variable. It can be hypointense on T1 and T2 sequences because of high cellularity and low water content. It can also be isointense in comparison to the parotid tissue on T2 and post-contrast

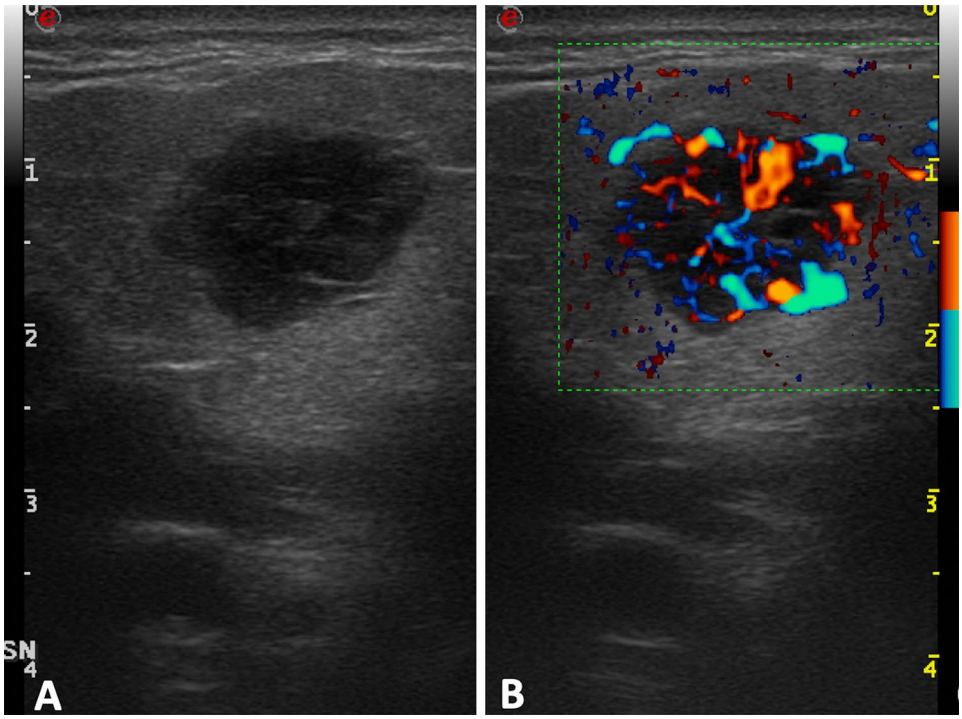

Fig. 4 B-mode **a** and color Doppler **b** ultrasound scans. Color Doppler shows lobulated, well-defined, and hypoechoic oncocytoma with a spoke-wheel pattern

T1 sequences (vanishing tumor) or even hypointense on T1 sequences with intermediate/low signal on T2 sequences [17, 25]. The signal intensity is also influenced by cystic and hemorrhagic areas or intralesional fat [26]. After the contrast medium injection, PGO usually shows a homogeneous enhancement [1, 6] (Fig. 5). MRI PGO features as well as CT ones overlap with those of Warthin's tumor. DWI imaging and ADC measurement results are highly useful in differentiating these two entities. In particular, on DWI, PGO shows lower signal intensity than Warthin's tumors, while ADC is lower in Warthin's tumors than PGO [8].

Positron emission tomography with F-18 fluorodeoxyglucose (PET-FDG) is useful in the evaluation and clinical management of head and neck lesions. However, regarding parotid tumors, its role is limited by a relatively high false-positive rate (approximately 30%), attributed mainly to Warthin's tumors. High FDG uptake has also been observed in oncocytomas, which may represent incidental findings in patients undergoing PET scans for other tumors (Fig. 6) [27–29]. In the setting of a cancer patient showing parotid gland focal uptake, further investigation is necessary to rule out a synchronous primary malignancy or a metastatic lesion. Hagino et al. hypothesized that the high FDG uptake observed in PGO is related to mitochondrial accumulation in oncocytic cells [29]. Furthermore, oncocytomas as well as Warthin's tumors concentrate pertechnetate unlike pleomorphic adenoma. Uchida et al. proposed a combination of salivary scintigraphy and PET-FDG to differentiate benign from malignant parotid tumors [27]. Scintigraphy should be performed first, and

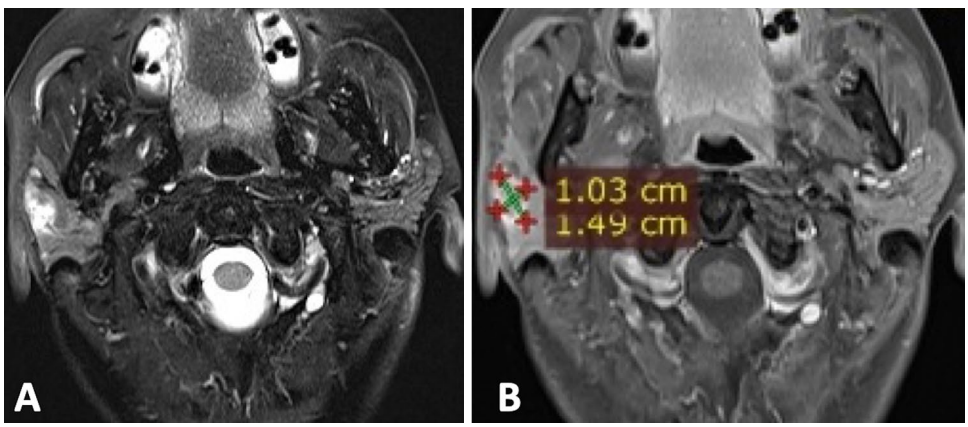

Fig. 5 T2-weighted **a** and post-contrast T1-weighted **b** axial MR images. Lobulated oncocytoma showing high signal intensity on T2w and post-contrast T1w images in the right parotid gland

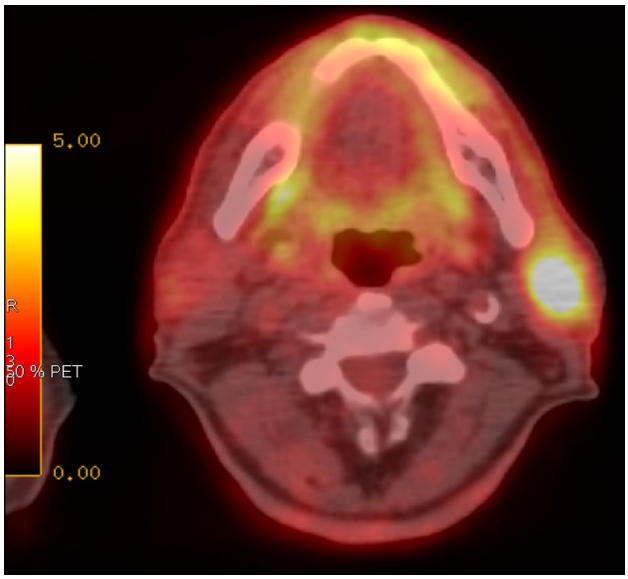

Fig. 6 PET-FDG. Oncocytoma of the left parotid gland showing increased FDG uptake

if negative, PET-FDG should be carried out as the subsequent step [29].

Further diagnostic workup and treatment options

Considering the significant overlap in morphological features among the various salivary lesions in cross-sectional imaging, FNAC or core biopsy are necessary to characterize the lesions before surgery [17]. These procedures are simple to perform, relatively risk free, and usually US guided because of their ready availability and ability to provide real-time images [30]. FNAC sensitivity and specificity in the assessment of salivary gland mass depend on operator expertise,in the literature, they range from 88 to 93% and from 75 to 99%, respectively [31, 32]. The reported sensitivity is much lower in detecting oncocytic neoplasia (29%), usually because of focal sampling of the lesion as oncocytic change can occur in a large variety of neoplastic as well as non-neoplastic conditions [6, 33]. Multiple passes may improve the cytologic diagnosis. However, FNAC does not allow one to differentiate PGO from oncocytic carcinoma, which is a histological diagnosis.

Surgical resection with facial nerve preservation represents the treatment of choice and the gold standard to acquire a precise diagnosis. The literature reports a local recurrence rate after surgery of 20–22% in the setting of residual tumor or multinodular cases, but malignant transformation has sometimes been reported [33, 34]. Thus, MRI after 1 and 2 years is strictly recommended to monitor for recurrence [6].

Conclusions

The diagnosis of PGO is challenging because of its rarity and overlapping with other tumors. An integrated clinical, imaging, and pathologic assessment is necessary to establish an accurate diagnosis. US plays an important role in the diagnostic workup of superficial lesions such as PGOs because it is a noninvasive, widely available, low-cost, well-tolerated, and non-ionizing radiation technique. The combination with Doppler techniques is important because the appearance of PGO in B-mode grayscale is similar to that of pleomorphic adenoma, but the high peak systolic flow and/or the spoke-wheel appearance may suggest an oncocytoma diagnosis. US has the unique advantage over other imaging techniques in providing real-time guidance for FNAC and biopsy, often necessary to confirm the diagnostic suspect. Hence, CT and MRI examination can be avoided in a similar setting.

Compliance with ethical standards

Conflict of interest We confirm that this work is original and has not been published elsewhere nor is it currently under consideration for publication elsewhere. Publication is approved by all authors and by the responsible authorities where the work was carried out. Each author have participated sufficiently in any submission to take public responsibility for its content. The authors have no conflicts of interest.

Informed consent Written informed consent was obtained from all patients, and the study was approved by the ethics committee of the institution.

References

1. Tan TJ, Tan TY (2010) CT features of parotid gland oncocytomas: A study of 10 cases and literature review. Am J Neuroradiol 31:1413–1417. https://doi.org/10.3174/ajnr.A2090
2. Sharma V, Kumar S, Sethi A (2018) Oncocytoma parotid gland. Ann Maxillofac Surg 8(2):330–332. https://doi.org/10.4103/ams.ams_154_17
3. Talas D, Go K (2006) Incidental deep lobe parotid gland oncocytic neoplasms in an operated larynx cancer patient. Oral Oncol Extra 42(6):235–240. https://doi.org/10.1016/j.ooe.2006.01.003
4. Madani G, Beale T (2006) Tumors of the Salivary Glands. Semin Ultrasound CT MRI 27(6):452–464. https://doi.org/10.1053/j.sult.2006.09.004
5. Hamada S, Fujiwara K, Hatakeyama H, Homma A (2018) Case report oncocytoma of the parotid gland with facial nerve paralysis. Case Rep Otolaryngol 2018:7687951. https://doi.org/10.1155/2018/76879512018:1-4
6. Sepúlveda I (2014) Oncocytoma of the parotid gland: a case report and review of the literature. Case Rep Oncol 4030000:109–116. https://doi.org/10.1159/000359998
7. Shellenberger TD, Williams MD, Clayman GL, Kumar AJ (2008) Parotid gland oncocytosis: ct findings with histopathologic

correlation. Am J Neuroradiol 29:734–736. https://doi.org/10.3174/ajnr.A0938
8. Kato H, Fujimoto K, Matsuo M, Mizuta K (2017) Usefulness of diffusion-weighted MR imaging for differentiating between Warthin ' s tumor and oncocytoma of the parotid gland. Jpn J Radiol. https://doi.org/10.1007/s11604-016-0608-5
9. Bialek EJ, Jakubowski W, Zajkowski P et al (2006) US of the major salivary glands: anatomy and spatial relationships, pathologic conditions, and pitfalls. RadioGraphics 26:745–763. https://doi.org/10.1148/rg.263055024
10. Orlandi MA, Pistorio V, Guerra PA (2013) Ultrasound in sialadenitis. J Ultrasound 16:3–9. https://doi.org/10.1007/s40477-013-0002-4
11. Valentino M, Quiligotti C, Carone L (2013) Branchial cleft cyst. J Ultrasound 16:17–20. https://doi.org/10.1007/s40477-013-0004-2
12. Corvino A, Pignata S, Campanino MR et al (2020) Thyroglossal duct cysts and site-specific differential diagnoses: imaging findings with emphasis on ultrasound assessment. J Ultrasound. https://doi.org/10.1007/s40477-020-00433-2
13. Catalano O, Roldán FA, Varelli C et al (2019) Skin cancer: findings and role of high-resolution ultrasound. J Ultrasound 22:423–431. https://doi.org/10.1007/s40477-019-00379-0
14. Corvino A, Sandomenico F, Corvino F et al (2020) Utility of a gel stand-off pad in the detection of Doppler signal on focal nodular lesions of the skin. J Ultrasound 23:45–53. https://doi.org/10.1007/s40477-019-00376-3
15. Caprio MG, Di Serafino M, Pontillo G et al (2019) Paediatric neck ultrasonography: a pictorial essay. J Ultrasound 22:215–226. https://doi.org/10.1007/s40477-018-0317-2
16. Lou L, Teng J, Lin X, Zhang H (2014) Ultrasonographic features of renal oncocytoma with histopathologic correlation. J Clin Ultrasound 42:129–133. https://doi.org/10.1002/jcu.22128
17. Cantisani V, David E, Sidhu P et al (2016) Parotid gland lesions: multiparametric ultrasound and mri features. Ultraschall Med 37(5):454–471. https://doi.org/10.1055/s-0042-109171
18. Martinoli C, Derchi LE, Solbiati L et al (1994) Color doppler sonography of salivary glands. Am J Roentgenol 163:933–941. https://doi.org/10.2214/ajr.163.4.8092039
19. Rubini A, Guiban O, Cantisani V, D'Ambrosio F (2020) Multiparametric ultrasound evaluation of parotid gland tumors: B-mode and color Doppler in comparison and in combination with contrast-enhanced ultrasound and elastography. A case report of a misleading diagnosis. J Ultrasound. https://doi.org/10.1007/s40477-020-00469-4
20. Săftoiu A, Gilja OH, Sidhu PS et al (2019) The EFSUMB guidelines and recommendations for the clinical practice of elastography in non-hepatic applications: Update 2018 TT - Die EFSUMB-Leitlinien und Empfehlungen für die klinische Praxis der Elastografie bei nichthepatischen Anwendungen: Update 20. Ultraschall Med 40:425–453. https://doi.org/10.1055/a-0838-9937
21. Mansour N, Bas M, Stock KF, Strassen U, Hofauer B, Knopf A (2017) Multimodal ultrasonographic pathway of parotid gland lesions multimodaler sonografischer diagnosepfad für parotisläsionen. Ultraschall Med 38(2):166–173. https://doi.org/10.1055/s-0035-1553267
22. Sidhu P, Cantisani V, Dietrich CF et al (2018) The EFSUMB guidelines and recommendations for the clinical practice of contrast-enhanced ultrasound (CEUS) in non-hepatic applications: Update 2017 (long version) die EFSUMB-Leitlinien und Empfehlungen für den klinischen Einsatz des kontrastverstärkten Ul. EFSUMB Guidel Ultraschall Med 39:2–44. https://doi.org/10.1055/a-0586-1107
23. Liu G, Wu S, Liang X et al (2018) Shear wave elastography improves specificity of ultrasound for parotid nodules. Ultrasound Q 34:62–66. https://doi.org/10.1097/RUQ.0000000000000354
24. Widziszowska A, Namysłowski G, Hajduk A, Lange D (2007) Przypadek gruczolaka kwasochłonnego śliniaki przyusznej penetrujacego do przestrzeni przygardłowej. Otolaryngol Pol 61:195–197. https://doi.org/10.1016/s0030-6657(07)70413-4
25. Patel ND, van Zante A, Eisele DW et al (2011) Oncocytoma: The vanishing parotid mass. Am J Neuroradiol 32:1703–1706. https://doi.org/10.3174/ajnr.A2569
26. Anzalone CL, Nagelschneider AA, Sims JR et al (2019) Oncocytoma presenting as a fat-containing intraparotid mass. Ear Nose Throat J 98:403–404. https://doi.org/10.1177/0145561319841210
27. Uchida Y, Minoshima S, Kawata T et al (2005) Diagnostic value of FDG PET and salivary gland scintigraphy for parotid tumors. Clin Nucl Med 30:170–176. https://doi.org/10.1097/00003072-200503000-00005
28. Shah VN, Branstetter BF (2007) Oncocytoma of the parotid gland: a potential false-positive finding on 18 F-FDG PET. Am J Roentgenol 189:W212–W214. https://doi.org/10.2214/AJR.05.1213
29. Hagino K, Tsunoda A, Ishihara A (2006) Oncocytoma in the parotid gland presenting a remarkable increase in fluorodeoxyglucose uptake on positron emission tomography. Case Rep. https://doi.org/10.1016/j.otohns.2005.03.076
30. Lee YYP, Wong KT, King AD, Ahuja AT (2008) Imaging of salivary gland tumours. Cancer Imaging 66:419–436. https://doi.org/10.1016/j.ejrad.2008.01.027
31. Jayaram G, Ak V, Sood N, Fine KN (1994) Fine needle aspiration cytoiogy of salivary gland lesions. J Oral Pathol Med 23(6):256–261
32. Corvino A, Catalano O, Corvino F, Sandomenico F, Setola SV, Petrillo A (2016) Superficial temporal artery pseudoaneurysm: what is the role of ultrasound? J Ultrasound 19(3):197–201. https://doi.org/10.1007/s40477-016-0211-8
33. Capone RB, Ha PK, Westra WH et al (2002) Oncocytic neoplasms of the parotid gland: A 16-year institutional review. Otolaryngol Neck Surg 126:657–662. https://doi.org/10.1067/mhn.2002.124437
34. Corvino A, Rosa D, Sbordone C, Nunziata A, Corvino F, Varelli C, Catalano O (2019) Diastasis of rectus abdominis muscles: patterns of anatomical variation as demonstrated by ultrasound. Pol J Radiol 84:e542–e548. https://doi.org/10.5114/pjr.2019.91303